VOLUME 111, NUMBER 18
AUGUST 30, 1989

JOURNAL
OF THE
AMERICAN
CHEMICAL
SOCIETY

Kinetic Titrations

Myron Kaufman

Contribution from the Department of Chemistry, Emory University, Atlanta, Georgia 30322.
Received December 22, 1988

Abstract: The equivalence point of the titration in a simple bimolecular reaction can be defined kinetically as the ratio of concentrations of reactants that results in maximum persistence of the reaction. This follows from the kinetics of the reaction remaining second-order at the stoichiometric ratio, whereas at any other ratio the reaction eventually becomes pseudo-first-order, with exponential decay of the limiting reagent. With allowance for axial diffusion, the shape of the titration curve can provide the rate constant of the titration reaction. The equivalence points for many titration reactions that proceed by mechanisms involving a series of reactions are predicted to be accurately indicated by the point of maximum persistence. However, some parallel reactions, such as wall or homogeneous loss of titrant or analyte, can distort the titration curve. Maximum persistence end points in agreement with theory are demonstrated for the O_3 + NO reaction, monitored by chemiluminescence in a low-pressure flow reactor.

A titration reaction

$$A + B \rightarrow \text{products} \qquad (I)$$

is a means of determining an amount of an analyte (A) by reacting it with an equivalent amount of titrant (B). Usually the titration reaction proceeds essentially to completion, so that its equivalence point can be identified as the amount of titrant (or the flow of titrant, if a steady flow of analyte is being determined) that must be added to the analyte so that neither titrant nor analyte remains. The assumption is usually made that the titration reaction is sufficiently rapid so that only the stoichiometry and not the kinetics of the titration reaction must be considered.

In the present work, an alternative approach to titration reactions, which explicitly focuses on their kinetics, is considered. In this approach the equivalence point of a titration reaction is identified as the ratio of titrant to analyte concentrations that results in "maximum persistence", i.e., maximum rate of the reaction at long times. At sufficiently long times, the reaction rate of a simple bimolecular reaction such as (I) is a very sharply peaked function of reactant ratio, allowing the equivalence point to be easily identified. This follows from a second-order reaction becoming pseudo-first-order if one of the reactants is present in great excess. As long as the reactants are not present in stoichiometric proportions, the limiting reagent will eventually be consumed to the point that its concentration will be much smaller than that of the other reagent. At times later than this, pseudo-first-order (exponential) decay of the limiting reagent will occur. Since at the stoichiometric ratio decay is second-order (proportional to $1/t$ at long times), the stoichiometric mixture will always decay more slowly than mixtures with any other proportion of reactants. Peaking of decay times at the stoichiometric ratio has also been reported in studies of relaxation kinetics.[1]

It will be shown that the titration curve can provide the rate constant of the titration reaction, as well as its equivalence point. Methods of experimentally observing the point of maximum persistence will be discussed, and the effect of diffusion on the results in flow systems will be considered. The results will be extended to titrations that proceed by a series of reactions, showing under what conditions a maximum persistence equivalence point is observed and exploring the shape of the titration curve for such reactions. Finally, parallel reactions will be considered, allowing the effect of first- and second-order loss of analyte to be evaluated. In the Experimental Section, agreement with theory is demonstrated for the NO + O_3 titration, monitored by chemiluminescence.

---

[1] Winkler-Oswatitsch, R.; Eigen, M. *Angew. Chem., Int. Engl. Ed.* **1979**, *18*, 20.

0002-7863/89/1511-6901$01.50/0

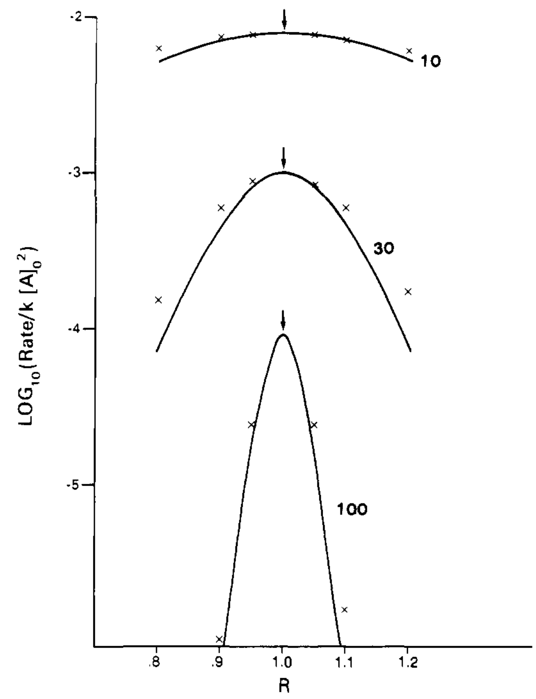

Figure 1. Curves: logarithm of the ratio of the reaction rate to the initial rate at the equivalence point as a function of the ratio of initial concentrations of reactants for a simple bimolecular titration reaction. Curves are given for $\mathcal{T} = k[\mathrm{A}]_0t$ = 10, 30, and 100. Diffusion is not included in these calculations. Crosses: corresponding quantities for a two-step mechanism with $k_1 = k_2$.

Theory

Case I: Simple Bimolecular Reaction. The rate equation for a simple bimolecular mechanism can be solved by the method of partial fractions,[2] to give

$$\ln \{[\mathrm{A}]_0([\mathrm{B}]_0 - x)/([\mathrm{B}]_0([\mathrm{A}]_0 - x))\} = k([\mathrm{B}]_0 - [\mathrm{A}]_0)t \qquad (1)$$

The rate of the reaction can then be written as

$$\text{rate} = k[\mathrm{A}]_0{}^2R\left[1 - \frac{(e^{(1-R)\mathcal{T}} - 1)}{(e^{(1-r)\mathcal{T}} - R)}\right]\left[1 - \frac{R(e^{(1-R)\mathcal{T}} - 1)}{(e^{(1-R)\mathcal{T}} - R)}\right] \qquad (2)$$

where $R = [\mathrm{B}]_0/[\mathrm{A}]_0$ and $\mathcal{T} = k[\mathrm{A}]_0t$.

The rate divided by $k[\mathrm{A}]_0{}^2$ is plotted as a function of R in Figure 1. The rate peaks very close to the stoichiometric ratio (within 0.4% at $\mathcal{T} = 10$, much closer at larger $\mathcal{T}$). The peak is not very sharp at $\mathcal{T} = 10$, but becomes increasingly sharp and reduced in intensity as $\mathcal{T}$ increases. Considering the logarithmic nature of the plots, the end point of the titration would be easily located at values of $\mathcal{T} \geq 30$. Since $\mathcal{T} = k[\mathrm{A}]_0t$ is known from the shape of the titration curve, $[\mathrm{A}]_0$ from its end point, and t from distance and velocity in the flow system, k can be determined from the titration. At times shorter than those plotted in Figure 1, the maximum shifts progressively to higher values of R. (When very little A is consumed, intensity is proportional to the concentration of B.) For $R = 1$, expression 2 is undefined, but the rate can be found using L'Hopital's rule to be $k[\mathrm{A}]_0{}^2/(1 + \mathcal{T})^2$, which at long time becomes $1/kt^2$, i.e., independent of $[\mathrm{A}]_0$. Thus, at a given time (or position in a flow reactor), as the concentration of analyte decreases, the signal at the end point of the titration remains constant, but becomes more difficult to discern since the titration curve becomes broader.

In order to determine the equivalence point of a reaction by the method of maximum persistence, the reaction must be monitored by a technique that measures a property nearly proportional to the instantaneous rate of reaction. Light emission by the product of a chemiluminescent reaction is such a property, if the emitter is lost (by radiation and quenching) on a time scale that is rapid compared to the characteristic time of the reaction. In addition, the method by which reaction rate is monitored must have sufficient sensitivity for measuring this rate at long times, when the rate has declined by at least three orders of magnitude from its initial value (see Figure 1). The great sensitivity of photodetectors in the visible and ultraviolet region, together with the possibility of using these detectors in pulse-counting modes, will often satisfy this sensitivity requirement. In fact, in several cases ($\mathrm{F + H_2}$[3] and $\mathrm{F + CH_3OH}$[4]), we have *visually* identified maximum persistence end points. Other techniques that might be explored as end-point indicators for the method of maximum persistence are measurement of the fluorescence of a reactive intermediate or the heat generated by the reaction (assuming that the characteristic time for heat transfer can be made shorter than the reaction time). Kinetic titrations are cumbersome to perform in the time domain, requiring that the time course of the titration reaction be repeatedly followed with varying ratio of initial concentrations. Alternatively, in a continuous flow reactor, a fixed detector at a distance d samples the reaction mixture at time $t = d/v$, where v is the linear flow velocity in the reactor (assuming plug flow).

Effect of Diffusion. In real reactors operating in the laminar-flow regime, plug flow is modified by a parabolic dependence of velocity on radius (assuming a circular cross section) and by axial and radial diffusion. The equations for a second-order reaction then become:

$$v_0(1 - r^2/r_0{}^2)\frac{\partial[\mathrm{A}]}{\partial x} = D\left(\frac{\partial^2[\mathrm{A}]}{\partial x^2} + \frac{\partial^2[\mathrm{A}]}{\partial r^2} + \frac{1}{\mathrm{r}}\frac{\partial[\mathrm{A}]}{\partial r}\right) - k[\mathrm{A}][\mathrm{B}] \qquad (3)$$

$$v_0(1 - r^2/r_0{}^2)\frac{\partial[\mathrm{B}]}{\partial x} = D\left(\frac{\partial^2[\mathrm{B}]}{\partial x^2} + \frac{\partial^2[\mathrm{B}]}{\partial r^2} + \frac{1}{r}\frac{\partial[\mathrm{B}]}{\partial r}\right) - k[\mathrm{A}][\mathrm{B}] \qquad (4)$$

where v_0 is the flow velocity at the center of the reactor of radius r_0. It is assumed that A and B have the same diffusion coefficient, D. Because we are considering distances along the length of the flow tube that are many times its diameter, it will be assumed that all radial concentration gradients are eliminated by diffusion. Replacing the parabolic velocity distribution by its area-average value, $v = v_0/2$, then gives

$$-v\frac{d[\mathrm{A}]}{\mathrm{d}x} + D\frac{\mathrm{d}^2[\mathrm{A}]}{d^2\mathrm{x}} = k[\mathrm{A}][\mathrm{B}] = -v\frac{\mathrm{d}[\mathrm{B}]}{\mathrm{d}x} + D\frac{\mathrm{d}^2[\mathrm{B}]}{\mathrm{d}x^2} \qquad (5)$$

or with $a = [\mathrm{A}]/[\mathrm{A}]_0$, $b = [\mathrm{B}]/[\mathrm{B}]_0$, $q = vx/D$, and $s = [\mathrm{A}]_0kD/v^2$ (s is a measure of the ratio of diffusive loss to reactive loss of the limiting reagent in the first-order regime.)

$$\frac{\mathrm{d}a}{\mathrm{d}q} = \frac{\mathrm{d}^2a}{\mathrm{d}q^2} - Rsab \qquad (6)$$

$$\frac{\mathrm{d}b}{\mathrm{d}q} = \frac{\mathrm{d}^2b}{\mathrm{d}q^2} - sab \qquad (7)$$

Equations 6 and 7 were converted to a set of four first-order differential equations and solved numerically by a difference equation method using IMSL program DVCPR.[5] The boundary conditions are $a = b = 1$ at $q_1 = 0$, and at a large value of q_2 (arbitrarily set to at least twice the largest value of interest), the

---

(2) See, for example: Skinner, G. B. *Introduction to Chemical Kinetics*; Academic Press: New York, 1974; p 19.

(3) Ganguli, P. S.; Hertzler, B. L.; Kaufman, M. *Chem. Phys. Lett.* **1976**, *37*, 319.

(4) Bogan, D. J.; Kaufman, M.; Sanders, W. A.; Hand, C. W.; Wang, H.-t. Proceedings of Eastern Section of Combustion Institute, Dec 1982.

(5) IMSL Inc., 2500 City West Blvd., Houston, TX 77042-3020.

Table I. −log (Rate/Rate$_{is}$) for a Bimolecular Reaction with Axial Diffusion

	R						
$\mathcal{T}$	0.8	0.9	0.95	1	1.05	1.1	1.2
$s = 0$							
10	2.26	2.13	2.10	2.08	2.09	2.12	2.24
30	4.10	3.31	3.07	2.98	3.07	3.30	4.08
60	6.70	4.65	3.88	3.57	3.88	4.64	6.69
100	10.03	6.39	4.79	4.01	4.79	6.38	10.03
$s = 0.2$							
10	2.17	2.06	2.03	2.02	2.02	2.05	2.15
30	3.96	3.24	3.03	2.95	3.02	3.24	3.94
60	6.47	4.57	3.85	3.55	3.84	4.56	6.45
100	9.82	6.27	4.75	3.99	4.74	6.27	9.80
$s = 0.5$							
10	2.06	1.97	1.95	1.94	1.94	1.96	2.03
30	3.78	3.16	2.98	2.91	2.97	3.16	3.76
60	6.20	4.46	3.80	3.52	3.79	4.45	6.16
100	9.49	6.12	4.69	3.97	4.68	6.11	9.42
$s = 1.0$							
10	1.95	1.87	1.85	1.84	1.84	1.86	1.90
30	3.58	3.06	2.90	2.84	2.90	3.06	3.55
60	5.82	4.32	3.73	3.48	3.73	4.31	5.79
100	8.78	5.91	4.61	3.95	4.60	5.91	8.75
$s = 2.0$							
10	1.77	1.72	1.70	1.69	1.69	1.70	1.72
30	3.30	2.91	2.78	2.74	2.78	2.90	3.26
60	5.30	4.10	3.61	3.41	3.61	4.08	5.26
100	7.94	5.58	4.47	3.90	4.47	5.58	7.91
$s = 5.0$							
10	1.50	1.47	1.46	1.45	1.44	1.44	1.44
30	2.84	2.62	2.55	2.53	2.55	2.60	2.80
60	4.47	3.69	3.38	3.25	3.38	3.68	4.44
100	6.62	4.98	4.18	3.78	4.18	4.96	6.58

limiting reagent concentration is set equal to zero and the other reagent to its excess. The results of the calculations for $\mathcal{T} = sq$ of interest, given in Table I, are found to be independent of considerable variation in q_2. With known D, k is determined by finding the value of s that best fits the shape of the titration curve at the experimental value of $x = D\mathcal{T}/sv$. In order to permit such fitting, an extensive table of rates as a function of $\mathcal{T}$ and s is given in the Supplementary Material.

The effect of including increasing amounts of diffusion in the calculation is to increase the reaction rate at any downstream point in the reactor as reagents diffuse from upstream. However, the effect of diffusion is relatively greater for ratios further from stoichiometric, since in these cases the limiting reagent concentration falls off much faster and thus provides a larger concentration gradient for diffusion. As a result, diffusion broadens the titration curves. Diffusion has very little effect on the end points of titrations, except at very low values of $\mathcal{T}$ and large amounts of diffusion, where the titration curve is almost flat.

Case II: **Two-Step Series Mechanism.** Persistent luminescence may also be observed in reactions that proceed by a multistep mechanism. Analysis of such systems may provide stoichiometric, mechanistic, and kinetic information. For example, consider the simple two-step series mechanism,

$$A + B \xrightarrow{k_1} Y$$

$$B + Y \xrightarrow{k_2} E$$

where E is an emitting product. When $k_1 \ll k_2$, the steady-state approximation for Y, $[Y] = k_1[A]/k_2$, holds, giving the kinetic equation

$$dx/dt = k_1([B]_0 - x)(2[A]_0 - x) \qquad (8)$$

where x is the concentration of B consumed. With the substitution of $2[A]_0$ for $[A]_0$, this is clearly the same equation as holds for the simple bimolecular mechanism (I). Thus, if for this two-step series mechanism at steady state, emission intensity is plotted against R', where $R' = [B]_0/2[A]_0$, for $\mathcal{T}' = 2k_1[A]_0t$, the curves would be identical with those shown in Figure 1.

In order to test the importance of the steady-state assumption for sharply peaked emission at the end point, the two-step series mechanism for $k_1 = k_2$, which clearly does not satisfy the steady-state condition, has been modeled using the Gear algorithm.[6] Results of this calculation are shown as crosses adjacent to the $\mathcal{T} = 30$ curve in Figure 1. Although there are small quantitative differences from the steady-state curves, the qualitative conclusion, that light emission at long times is sharply peaked at the stoichiometric concentration ratio, is still valid.

For the two-step mechanism, it is also possible to consider the limit $k_1 \gg k_2$. In this case, the first reaction goes rapidly to completion, consuming $[A]_0$ of B. Luminescence from the second reaction then peaks at its equivalence point, when a second $[A]_0$ of B is consumed. Light emission at long times is again strongly peaked at the equivalence point of the overall reaction ($[B]_0 = 2[A]_0$). However, the variation of luminescence around the equivalence point is now determined by the value of $\mathcal{T}' = k_2[A]_0t$, since reaction 2 is rate limiting, and $[A]_0$ of Y must react at the equivalence point of this reaction. In this case, $R' = ([B]_0 - [A]_0)/[A]_0$, and no light is emitted in the first half of the titration. Such differences in the shape of the titration curve may allow mechanisms to be distinguished by studying persistent luminescence. Although we have not attempted a general proof, it appears that in the two-step series mechanism, long-time light emission will always peak very close to the equivalence point of the reaction.

Case III: General Series Mechanism. It is also possible to draw some conclusions regarding a general n-step series mechanism, of the form

$$A + B \xrightarrow{k_1} Y_1$$

$$B + Y_1 \xrightarrow{k_2} Y_2$$

$$B + Y_2 \xrightarrow{k_3} Y_3 \text{ etc.}$$

Only the case in which one reaction in the series is much slower than all the others will be discussed. If the first reaction in this mechanism is rate limiting, n B's will be consumed simultaneously for each A that reacts. Thus if the variables $R' = [B]_0/n[A]_0$ and $\mathcal{T}' = nk_1[A]_0t$ are employed, this mechanism gives curves identical with those shown in Figure 1, regardless of which intermediate emits light.

If the initial reaction is not rate limiting, the results depend upon whether the rate-limiting reaction in the series comes before or after the production of the luminescent species. If the rate-limiting step comes before the production of the luminescent product, say after n' steps, $n'[A]_0$ B's will be rapidly consumed with no luminescence, and all the initial A will be rapidly converted to $Y_{n'}$. As more B is added, subsequent Y's will be in steady state with $Y_{n'}$ and will all be formed at maximum long-term rates when just an additional $(n - n')[A]_0$ of B is available. Once again maximum long-term emission will occur at the overall equivalence point, $[B]_0 = n[A]_0$. The variation of the emission around the end point will now be determined by the value of $\mathcal{T}' = (n - n')k_{n'+1}[A]_0t$ and is in the variable $R' = ([B]_0 - n'[A]_0)/((n - n')[A]_0)$. If, however, the rate-limiting step occurs after the formation of the luminescent intermediate, the buildup of the slowly reacting intermediate will result in pseudo-first-order decay of B, and no persistent luminescence will be observed. It is suggested by these considerations and the modeling for $k_1 = k_2$ in the two-step mechanism that, if persistent luminescence is observed in a series of reactions, maximum persistence should occur at the equivalence point of the overall reaction.

Case IV: Parallel Mechanisms. One important parallel mechanism is

---

[6] Gear, C. W. *Numerical Initial Value Problems in Ordinary Differential Equations*; Prentice-Hall: Englewood Cliffs, NJ, 1971.

$$A + B \xrightarrow{k_1} E$$

$$A \xrightarrow{k_2} P$$

This mechanism holds when either analyte or titrant are consumed by a wall reaction. Noting that

$$d[A]/d[B] = (k_1[B] + k_2)/k_1[B] \tag{9}$$

we obtain

$$[A] = [A]_0 + ([B] - [B]_0) + (k_2/k_1) \ln ([B]/[B]_0) \tag{10}$$

which when substituted into $d[B]/dt = -k_1[A][B]$, with $R = [B]_0/[A]_0$, $b = [B]/[B]_0$, and $h = k_2/(k_1[B]_0)$, gives

$$k_1[B]_0t = \int_b^1 db'/(b'(1/R + (b'-1) + h \ln b')) \tag{11}$$

This equation has been numerically integrated using Simpson's rule, showing that if $h < 10^{-3}$, the results are indistinguishable from the curves in Figure 1. However, for $h = 10^{-2}$ the differences from Figure 1 are substantial. For titrations involving stable molecular analytes and titrants, these considerations will generally not be important. For atoms and radicals, undistorted titration curves will usually be achieved in cases in which the titration reactions are fast and the walls can be treated to avoid loss of the analyte.

Another parallel mechanism of interest involves two competing second-order reactions:

$$A + B \xrightarrow{k_1} E$$

$$A + A \xrightarrow{k_2} P$$

This mechanism would hold, for example, if an analyte undergoes homogeneous recombination simultaneously with being titrated. In this case, if

$$[B]/[A] = 1 - k_2/k_1 \tag{12}$$

then

$$d[A]/d[B] = (k_1[B] + k_2[A])/(k_1[B]) = [A]/[B] \tag{13}$$

and the ratio of A to B will not change, resulting in second-order kinetics and maximum persistence. Thus, the end point of this titration will be displaced by an amount k_2/k_1 from the equivalence point of the first reaction. The titration curve will be asymmetric, since with excess [A], A will decay relatively faster than B until (12) is reached, after which decay will be by second-order kinetics. However, with any excess B, the reaction will tend toward pseudo-first-order decay.

The final mechanism considered is

$$A + B \xrightarrow{k_1} E$$

$$B + C \xrightarrow{k_2} P$$

This mechanism is important, for example, if there is an impurity in the system that reacts with the titrant. If in this mechanism, $k_2 < k_1$, C will persist at long times and eventually the decay of B will become pseudo-first-order. Thus, simultaneous decay of A and B will not be possible. Of course, whether persistent decay of luminescence is perceived or not will depend on the relative rates of the two reactions and the relative concentrations of A and C. A very small concentration of a very slowly reacting "impurity" will clearly have little effect on the titration.

If $k_2 > k_1$, reaction with C will be essentially complete before the end point is reached, and maximum persistence will be achieved when $[B]_0 = [A]_0 + [C]_0$. In this case the variation of intensity around the end point will be determined by the value of $\mathscr{J} = k_1[A]_0t$ and be in the variable $R' = ([B]_0 - [C]_0)/[A]_0$.

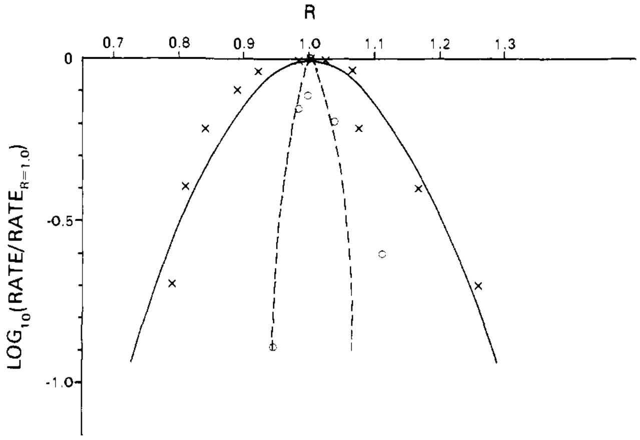

Figure 2. Points: logarithim of the ratio of the measured chemiluminescence of the NO + O_3 reaction to the peak value of chemiluminescence as the ratio of NO to O_3 (R) is varied. Curves, theory for comparison with experiment: (—) at $\mathscr{J} = 21.3$, $s = 0.36$; (---) at $\mathscr{J} = 99.6$, $s = 2.2$.

Comparison with Experiment. The chemiluminescent reaction of O_3 with NO was chosen for comparison with theory since it is known to produce emitting NO_2 by the simple mechanism:[7]

$$O_3 + NO \xrightarrow{k_{II}} NO_2 + O_2 \tag{II}$$

$$O_3 + NO \xrightarrow{k_{III}} NO_2{}^* + O_2 \tag{III}$$

$$NO_2{}^* \xrightarrow{k_r} \text{light} \tag{IV}$$

$$NO_2{}^* + M \xrightarrow{k_q} NO_2 + M \tag{V}$$

Reactions II and V do not complicate the analysis, but do reduce the intensity of the photosignal, as does the poor overlap of the sensitivity of the phototube with the spectral distribution of the chemiluminescence, which peaks at ca. 1300 nm.[8] The overall rate constant, $k_{II} + k_{III}$, reported to be $2.0 \pm 0.2 \times 10^{-14}$ cm^3 $molecule^{-1}$ s^{-1},[9] is used in the case I analysis. Besides its simple mechanism, added advantages of the O_3 + NO reaction as a prototype are that wall reactions are probably negligible and that the diffusion coefficients of the reagents do not differ greatly.

Titrations of O_3, at concentrations of 3.6×10^{14} and 1.8×10^{15} cm^{-3} in O_2, are shown in the logarithimic curves of Figure 2. For the diffusion coefficient (which should be the average of values for O_3 and NO in O_2), a value of 33 cm^2 s^{-1} at 4.3 Torr is employed.[10] The two runs correspond to $\mathscr{J} = 21.3$, $s = 0.36$ and $\mathscr{J} = 99.6$, $s = 2.2$, respectively. As predicted by the case I theory, the peak intensity of the titration curve is found to vary less than 10% with initial concentrations of ozone varying by more than a factor of 4.

Notwithstanding the considerable scatter of the experimental points, due to the weak photosignal and the difficulty in measuring the very small variations in flow of the NO titrant, the agreement between theory and experiment is quite satisfactory. Thus the theory seems adequate for the present experiments. A simple change in the theory, which might be appropriate for more precise data or for experiments involving reactants of very different size, would be to use different diffusion constants on each side of the equivalence point. (The constant for the limiting reagent in each regime should be employed.)

---

[7] Clyne, M. A. A.; Thrush, B. A.; Wayne, R. P. *Trans. Faraday Soc.* **1964**, *60*, 359.

[8] Kenner, R. D.; Ogryzlo, E. A. In *Chemi- and Bioluminescence* Bur, J. G., Ed.; M. Dekker, New York, 1985; p 137.

[9] Michael, J. V.; Allen, J. E., Jr.; Brobst, W. D. *J. Phys. Chem.* **1981**, *85*, 4109.

[10] For O_3 in O_2: Houzelot, J. L.; Villemaux, J. *J. Chim. Phys. Phys.-Chim. Biol.* **1977**, *74*, 229. For NO in O_2, an experimental value for CO in O_2 is used from: Hirschfelder, J. O.; Curtiss, C. F.; Bird, R. B. *Molecular Theory of Gases and Liquids*; Wiley: New York, 1954; p 579.

Another system in which persistent luminescence has been observed is F_2 + NO, where light, presumably from FNO,[11] peaks at $[NO]_0 = 2[F_2]_0$. As previously mentioned, sharply peaked downstream emission has also been observed in the F + H_2[3] and F + CH_3OH[4] reactions. These systems are all more complicated than O_3 + NO, containing possibilities of series and parallel reactions. Their detailed analysis has not yet been completed.

Experimental Section

Chemiluminescence from the NO + O_3 reaction was studied in a 2-in. diameter Teflon-coated Pyrex flow tube at 25 °C and 4.3 Torr with luminescence observed ca. 70 cm downstream of the mixing zone by a cooled R406 photomultiplier. The flow velocity was 25 cm/s. A steady flow of ozone was obtained in O_2 diluent by directing the output from a Wellsbach Model T406 ozonizer directly into the flow tube. At full voltage the ozonizer produces ca. 2% ozone, at which concentration the titration is too sharply peaked to give a meaningful comparison with theory. However, when the voltage of the ozonizer is reduced to 60–75 V, it produces ca. 0.25–1.25% O_3 (as measured by the end point of the titration) and gives the titration curves shown in Figure 2. Nitric oxide (Linde) was taken directly from a lecture bottle. Its flow was adjusted by means of a Granville-Phillips metal seal series 203 variable leak. The flow from the ozonizer was measured by a Brooks mercury piston flowmeter and that of NO by directing the flow into an evacuated calibrated volume and measuring the rate of pressure increase in the volume. System pressure was measured with a 0–100 Torr MKS Baratron gauge. Flows were permitted to stabilize for several hours before taking measurements.

Acknowledgment. The author thanks Dr. A. Fontijn for several helpful conversations dealing with this work. Support of this work by the Air Force Office of Scientific Research is gratefully acknowledged.

Supplementary Material Available: Table of rates as a function of ϑ and s (5 pages). Ordering information is given on any current masthead page.

---

(11) Johnston, H. S.; Bertin, H. J., Jr. *J. Mol. Spectrosc.* **1959**, *3*, 683.

Conformational Analysis. 12. 2-Chloropropenoyl Chloride. An Electron-Diffraction Investigation of the Molecular Structure, Conformational Composition, Anti–Syn Energy and Entropy Differences, and Potential Hindering Internal Rotation

Kolbjørn Hagen and Kenneth Hedberg*

Contribution from the Departments of Chemistry, AVH, University of Trondheim, N-7055 Trondheim, Norway, and Oregon State University, Corvallis, Oregon 97331-4003.

Received January 12, 1989

Abstract: The molecular structure of 2-chloropropenoyl chloride ($CH_2{=}CCl{-}C{=}OCl$) has been investigated at three temperatures by gas-phase electron diffraction. Two conformers were identified, a more stable anti form and a less stable planar (or near planar) syn form. The mole fractions of the anti form with uncertainties estimated at 2σ were found to be 0.775 (98) at 303 K, 0.704 (71) at 377 K, and 0.660 (75) at 475 K and correspond to $\Delta E° = E_s° - E_a° = 3.8(\sigma{=}2.2)$ kJ·mol^{-1} and $\Delta S_s° = S_s° - S_a° = 2.7(\sigma{=}5.6)$ J·mol^{-1}·K^{-1}. The energy difference and the root-mean-square torsional amplitudes for the two conformers were used to calculate a torsional potential of the form $2V = \sum V_i(1 - \cos i\phi)$ through three terms. The results are $V_1 = 2.1(\sigma{=}1.3)$, $V_2 = 7.5(\sigma{=}1.2)$, and $V_3 = 1.7(\sigma{=}0.3)$, all in kJ·mol^{-1}. No temperature dependence of the distances and angles was found. The following values, with estimated 2σ uncertainties, of the principal bond distances (r_g) and bond angles ($\angle_\alpha$) are for a "best model" comprising averages of the results from the three temperatures. (The atom numbering corresponds to the arrangement $C_1{=}C_2{-}C_3$; except for $\angle C_2{-}C_3{-}Cl$ and the torsion angles, the parameter values for the anti and syn forms were assumed equal.) $r(C_3{=}O) = 1.189$ (2) Å, $r(C{=}C) = 1.342$ (3) Å, $r(C{-}C) = 1.496$ (3) Å, $\langle r(C{-}Cl)\rangle = 1.753$ (2) Å, $\Delta r(C{-}C) = r(C_3{-}Cl) - r(C_2{-}Cl) = 0.041$ (6) Å, $r(C_3{-}Cl) = 1.774$ (4) Å, $r(C_2{-}Cl) = 1.733$ (4) Å, $\angle C{-}C{=}O = 125.5$ (6)°, $\angle C{=}C{-}C = 122.0$ (6)°, $\angle C_3{-}C_2{-}Cl = 118.3$ (4)°, $\langle \angle C_2{-}C_3{-}Cl\rangle = 113.4$ (3)°, $\Delta\angle C_2{-}C_3{-}Cl = \angle C_2{-}C_3{-}Cl(\text{syn}) - \angle C_2{-}C_3{-}Cl(\text{anti}) = 3.0°$ (assumed). The conformations of the molecule are discussed in relation to those of similar molecules.

Substitution of the aldehyde proton in conjugated aldehydes with a halogen atom has been shown to affect strongly the relative energies of the rotational conformers. In gaseous propenal[1] ($CH_2{=}CH{-}CH{=}O$) the form with the double bonds anti to each other predominates, and the energy difference $\Delta E_{s-a}° = E_s° - E_a°$ was measured to be 7.11 ± 0.17 kJ·mol^{-1}. For gaseous propenoyl chloride[2] and propenoyl fluoride[3] ($CH_2{=}CH{-}CX{=}O$) substantially greater proportions of the syn conformer are present, with $\Delta E_{s-a}° = 1.0 \pm 1.7$ kJ·mol^{-1} and 0.42 ± 0.08 kJ·mol^{-1}, respectively. For fumaraldehyde[4] ($O{=}CH{-}CH{=}CH{-}C{=}O$) only the anti–anti conformer was observed, but in fumaryl chloride[5] ($O{=}CCl{-}CH{=}CH{-}CCl{=}O$) three different conformers (anti–anti, anti–syn, and syn–syn) with about equal energies were identified.

Our investigations of conjugated systems are intended to provide the structural data that will permit a better understanding of the conformational behavior of such systems. 2-Chloropropenoyl chloride (Figure 1; hereafter CPC) is an especially interesting case because of its structural similarity to 2,3-dichloro-1,3-butadiene,[6] oxalyl chloride,[7] and propenoyl chloride,[2] which have different conformational properties: although the more stable form is the anti form in each case, the second form in 2,3-dichloro-1,3-butadiene and oxalyl chloride is gauche (respectively about 15% and 60% at high temperatures), but in propenoyl chloride it is planar or near planar syn. We had expected the conformers of CPC to

---

(1) Blom, C. E.; Grassi, G.; Bauder, A. *J. Am. Chem. Soc.* **1984**, *106*, 7427. Blom, C. E.; Bauder, A. *Chem. Phys. Lett.* **1982**, *88*, 55.

(2) Hagen, K.; Hedberg, K. *J. Am. Chem. Soc.* **1984**, *106*, 6150.

(3) Durig, J. R.; Church, J. S.; Compton, D. A. C. *J. Chem. Phys.* **1979**, *71*, 1175.

(4) Paulen, G.; Traetteberg, M. *Acta Chem. Scand.* **1975**, *A28*, 1155.

(5) Hagen, K. *J. Mol. Struct.* **1985**, *128*, 139.

(6) Hagen, K.; Hedberg, K.; Neisess, J.; Gundersen, G. *J. Am. Chem. Soc.* **1985**, *107*, 341.

(7) Hagen, K.; Hedberg, K. *J. Am. Chem. Soc.* **1973**, *95*, 1003.